

Strong-coupling limit of a Kondo spin coupled to a mesoscopic quantum dot: Effective Hamiltonian in the presence of exchange correlations

Stefan Rotter¹ and Y. Alhassid²

¹*Institute for Theoretical Physics, Vienna University of Technology, A-1040 Vienna, Austria*

²*Center for Theoretical Physics, Sloane Physics Laboratory, Yale University, New Haven, Connecticut 06520, USA*

(Received 30 July 2009; published 2 November 2009)

We consider a Kondo spin that is coupled antiferromagnetically to a large chaotic quantum dot. Such a dot is described by the so-called universal Hamiltonian and its electrons are interacting via a ferromagnetic exchange interaction. We derive an effective Hamiltonian in the limit of strong Kondo coupling, where the screened Kondo spin effectively removes one electron from the dot. We find that the exchange-coupling constant in this reduced dot (with one less electron) is renormalized and that additional interaction terms appear beyond the conventional terms of the strong-coupling limit. The eigenenergies of this effective Hamiltonian are found to be in excellent agreement with exact numerical results of the original model in the limit of strong Kondo coupling.

DOI: 10.1103/PhysRevB.80.184404

PACS number(s): 72.15.Qm, 72.10.Fk, 73.21.La, 73.23.Hk

I. INTRODUCTION

The Kondo effect, which emerges when a localized impurity spin interacts antiferromagnetically with a delocalized electron gas, has generated considerable interest since it was first described in 1964.^{1,2} The observation that the Kondo resonance can be realized in the mesoscopic regime of quantum dots, in which many of the system parameters are experimentally tunable, has led to much renewed interest over the last decade.^{3–13} This experimental work has been accompanied by substantial theoretical progress on the mesoscopic aspects of the Kondo problem.^{14–27}

In the mesoscopic regime, the spin-1/2 Kondo impurity is typically represented by a small quantum dot with an odd number of electrons while the delocalized electron gas is realized by electrons in leads or in a large quantum dot. In this work we focus on the latter case, assuming two quantum dots of different size that are coupled antiferromagnetically, as in Fig. 1(a) (see Ref. 9 for an experimental realization of such a setup).

Certain features distinguish the mesoscopic Kondo regime from the bulk limit. While the conventional Kondo theory assumes a continuum band of energy levels in the electron gas, the single-particle energy levels in the large quantum dot are discrete. The discreteness and the dot-specific realization of these energy levels become important when the Kondo temperature T_K , the characteristic energy scale of the correlated Kondo resonance, is of the same order of magnitude as or smaller than the average level spacing $\bar{\delta}$.^{17,19,23,24,27} In the conventional bulk Kondo model the electron-electron interactions in the electron gas are often neglected. However, for the present double-dot setup, electron-electron interactions in the large dot can play an important role. In the following we assume the single-particle dynamics in the large quantum dot to be chaotic,^{28–31} in which case the dot is described by the so-called “universal Hamiltonian.”³² This Hamiltonian describes the low-energy physics in a Thouless energy interval around the dot’s Fermi energy. For a semiconductor quantum dot with a fixed number of electrons and in the limit of a large Thouless conductance, the electron-electron interaction is dominated by a ferromagnetic exchange interaction that is

proportional to the square of the total dot’s spin. The universal Hamiltonian was shown to yield a quantitative agreement³³ with experimental results measuring the statistics of the Coulomb-blockade peak heights and spacings.³⁴

The effect of ferromagnetic exchange correlations on the Kondo resonance was first addressed analytically in the bulk limit³⁵ and, more recently, mean-field studies were carried out in the mesoscopic regime.²³ In a recent work, we studied this problem numerically and provided analytical results for the weak and strong Kondo coupling limits.²⁷ We found that for weak Kondo coupling, the Kondo spin acts like an external magnetic field, assisting the ferromagnetic polarization of

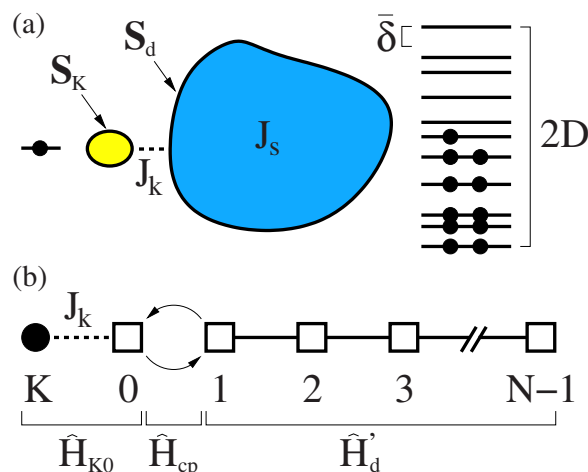


FIG. 1. (Color online) (a) Schematic illustration of the system under consideration: a small quantum dot with spin S_K (Kondo spin) is coupled antiferromagnetically (coupling constant J_k) to a large quantum dot with spin S_d . The large dot is described by the universal Hamiltonian, characterized by a ferromagnetic exchange interaction (coupling constant J_s). The N single-particle energy levels in the large dot are distributed within a band of width $2D$ (half filling). The average single-particle level spacing is fixed and given by $\bar{\delta}$. (b) The large dot is represented in the site basis (squares), in which S_K couples only to site 0. In the strong-coupling limit, $J_k \rightarrow \infty$, it is useful to divide the Hamiltonian into three parts, \hat{H}_{K0} , \hat{H}_{cp} , and \hat{H}'_d [see Eq. (8)].

electrons in the large dot. In the case of strong Kondo coupling, the Kondo spin effectively removes one of the electrons of the large dot. We showed that this “reduced” dot with one less level and one less electron can again be described by a universal Hamiltonian but with a renormalized exchange constant.

A central issue that was not addressed in our previous work concerns the nature of residual interactions in the reduced dot beyond the renormalization of its exchange interaction term. From the work of Nozières³⁶ we know that a noninteracting electron gas turns into a Fermi liquid when strongly coupled to a Kondo spin. The dominant effective interaction between the quasiparticles in this Fermi liquid is a repulsive interaction between spins of opposite orientation that are in close proximity to the Kondo spin. In the present case, the finite exchange interaction in the large dot leads to additional effective interaction terms in the strong-coupling limit. To identify these interaction terms, we follow a strategy that is similar to the one used by Nozières,³⁶ i.e., we perform an explicit perturbative expansion of the effective Hamiltonian of the reduced dot in the strong-coupling limit. In the presence of exchange interaction, this strong-coupling expansion is significantly more involved. However, the resulting effective quasiparticle interaction contains only a few new terms. The analytical expressions we derived for these effective exchange-like interactions are validated by a comparison with a full numerical diagonalization of the original two-coupled-dots model.

The outline of this paper is as follows: in Sec. II we present the model of a spin-1/2 quantum dot that is Kondo coupled to a large quantum dot (described by the universal Hamiltonian), and discuss the transformation from the single-particle orbital basis of the large dot to a chain site basis, commonly employed in the strong-coupling limit. In Sec. III we discuss the limit of strong Kondo coupling and use a projection method to derive an effective Hamiltonian for the reduced large quantum dot with one less electron. In Sec. IV we describe the evaluation of the eigenenergies of this effective Hamiltonian and in Sec. V we compare the results derived from this effective Hamiltonian with an exact numerical solution of the original model. In Sec. VI we conclude with a summary and discussion.

II. MODEL

We consider a chaotic quantum dot that is coupled antiferromagnetically to a Kondo spin as realized, e.g., by a small quantum dot with an odd number of electrons. A schematic illustration of such a system is shown in Fig. 1(a). In the following we will refer to the large quantum dot as the “dot” and to the small dot as the “Kondo spin.”

A. Hamiltonian

In the limit of a large Thouless conductance, a quantum dot whose single-particle dynamics are chaotic is described by the universal Hamiltonian³²

$$\hat{H}_d = \sum_{n=0}^{N-1} \sum_{\sigma} \varepsilon_n^{\sigma} \hat{a}_{n,\sigma}^{\dagger} \hat{a}_{n,\sigma} - J_s \hat{\mathbf{S}}_d^2. \quad (1)$$

Here $\hat{a}_{n,\sigma}^{\dagger}$ creates an electron with spin up/down ($\sigma = \pm 1$) in level n in an orbital single-particle level with energy ε_n^{σ} . We

assume N spin-degenerate single-particle levels spanning a bandwidth of $2D = (N-1) \times \bar{\delta}$ ($\bar{\delta}$ is the mean level spacing). The second term on the right-hand side (rhs) of Eq. (1) represents a ferromagnetic exchange interaction ($J_s > 0$), where $\hat{\mathbf{S}}_d = \frac{1}{2} \sum_{n\sigma\sigma'} \hat{a}_{n\sigma}^{\dagger} \boldsymbol{\tau}_{\sigma\sigma'} \hat{a}_{n\sigma'}$ ($\boldsymbol{\tau}$ are Pauli matrices) is the total spin of the dot. In Eq. (1) we have ignored a constant charging energy term and a repulsive Cooper channel term.

The dot is coupled antiferromagnetically to a Kondo spin $\hat{\mathbf{S}}_K$ ($S_K = 1/2$) (Ref. 23)

$$\hat{H} = \hat{H}_d + J_k \hat{\mathbf{S}}_K \cdot \hat{\mathbf{s}}_d(0), \quad (2)$$

where J_k ($J_k > 0$) is the Kondo coupling constant and $\hat{\mathbf{s}}_d(0)$ is the spin density of the dot at the tunneling position $\mathbf{r}=0$. The dot spin density at position \mathbf{r} is given by

$$\hat{\mathbf{s}}_d(\mathbf{r}) = \frac{1}{2} \sum_{\sigma,\sigma'} \hat{\psi}_{\sigma}^{\dagger}(\mathbf{r}) \boldsymbol{\tau}_{\sigma,\sigma'} \hat{\psi}_{\sigma'}(\mathbf{r}), \quad (3)$$

where $\hat{\psi}_{\sigma}^{\dagger}(\mathbf{r})$ creates an electron with spin σ at position \mathbf{r} . In terms of the single-particle orbital wave functions $\phi_n(\mathbf{r})$, the field operator is given by $\hat{\psi}_{\sigma}^{\dagger}(\mathbf{r}) = \sum_{n=0}^{N-1} \phi_n(\mathbf{r}) \hat{a}_{n,\sigma}^{\dagger}$ and the local density of states of the dot is given by^{17,23,24} $\rho(\varepsilon) = \sum_{n=0}^{N-1} |\phi_n(0)|^2 \delta(\varepsilon - \varepsilon_n^{\sigma})$, with an average value of $\bar{\rho} \approx 1/(N\bar{\delta})$.

B. Chain site basis

The strong-coupling limit of the system in Fig. 1(a) is more clearly described when the Hamiltonian in Eq. (2) is rewritten in a different basis, known as the chain site basis. This chain site basis is obtained by a unitary transformation of the orbital basis²

$$\hat{c}_{\mu,\sigma}^{\dagger} = \sum_{n=0}^{N-1} U_{\mu,n} \hat{a}_{n,\sigma}^{\dagger}, \quad (4)$$

such that site $\mu=0$ corresponds to the tunneling position $\mathbf{r}=0$, and the one-body site Hamiltonian of the dot is now tridiagonal, i.e., each site is coupled to its two nearest neighbors. Such a transformation is constructed by choosing $\hat{c}_{\mu=0,\sigma}^{\dagger} \equiv \hat{\psi}_{\sigma}^{\dagger}(\mathbf{r}=0)$ and carrying out a Gram-Schmidt orthogonalization procedure.²

The site single-particle energies $\varepsilon_{\mu}^{\sigma}$ are given by the diagonal elements of $\hat{H}_0 = \sum_{n=0}^{N-1} \sum_{\sigma} \varepsilon_n^{\sigma} \hat{a}_{n,\sigma}^{\dagger} \hat{a}_{n,\sigma}$ when the latter is rewritten in the site basis. The off-diagonal matrix elements $t_{\mu} \equiv t_{\mu,\mu+1}$ and $t_{\mu}^* \equiv t_{\mu,\mu-1}$ describe the hopping amplitudes between neighboring sites. A spin $\hat{\mathbf{s}}_{\mu}$ can be associated with each site, where the spin of site $\mu=0$ is equal to the spin density at the tunneling position, i.e., $\hat{\mathbf{s}}_0 \equiv \hat{\mathbf{s}}_d(0)$. In the site basis, the Kondo spin couples only to a single site $\mu=0$. The Hamiltonian in Eq. (2) is now given by

$$\hat{H} = \hat{H}_0 - J_s \hat{\mathbf{S}}_d^2 + J_k \hat{\mathbf{S}}_K \cdot \hat{\mathbf{s}}_0, \quad (5)$$

where the total spin of the dot is $\hat{\mathbf{S}}_d = \sum_{\mu=0}^{N-1} \hat{\mathbf{s}}_{\mu}$. Here \hat{H}_0 is the one-body Hamiltonian of the dot in the site basis

$$\hat{H}_0 = \sum_{\mu=0}^{N-1} \sum_{\sigma} \varepsilon_{\mu}^c \hat{c}_{\mu\sigma}^{\dagger} \hat{c}_{\mu\sigma} + \hat{H}_{\text{hop}}, \quad (6)$$

with \hat{H}_{hop} being the hopping Hamiltonian

$$\hat{H}_{\text{hop}} = \sum_{\mu=0}^{N-2} \sum_{\sigma} (t_{\mu} \hat{c}_{\mu,\sigma}^{\dagger} \hat{c}_{\mu+1,\sigma} + \text{H.c.}). \quad (7)$$

The site-basis formulation is particularly advantageous for the strong-coupling limit $J_k \rightarrow \infty$ when the site $\mu=0$ effectively decouples from the rest of the chain. Accordingly, we decompose the Hamiltonian in Eq. (5) into three terms [see Fig. 1(b) for a schematic illustration]

$$\hat{H} = \hat{H}_{K0} + \hat{H}'_d + \hat{H}_{cp}, \quad (8)$$

where H_{K0} describes the Hamiltonian of the Kondo spin plus site $\mu=0$, \hat{H}'_d is the Hamiltonian of a “reduced” dot with $N-1$ sites $\mu=1, \dots, N-1$, and \hat{H}_{cp} contains the remaining coupling terms. Writing $\hat{S}_d = \hat{S}'_d + \hat{s}_0$, where $\hat{S}'_d = \sum_{\mu=1}^{N-1} \hat{S}_{\mu}$ is the spin of the reduced dot, we have

$$\hat{H}_{K0} = \varepsilon_0^c \hat{n}_0 - J_s \hat{s}_0^z + J_k \hat{S}_K \cdot \hat{s}_0, \quad (9)$$

$$\hat{H}'_d = \hat{H}_0 - J_s \hat{S}'_d{}^2, \quad (10)$$

$$\hat{H}_{cp} = -2J_s \hat{s}_0 \cdot \hat{S}'_d + \sum_{\sigma} (t_0 \hat{c}_{0,\sigma}^{\dagger} \hat{c}_{1,\sigma} + \text{H.c.}). \quad (11)$$

\hat{H}'_d in Eq. (10) is the “bare” Hamiltonian of the reduced dot given by expressions similar to Eqs. (6) and (7) but with the sums over μ starting at $\mu=1$.

Here and in the following, operators in the reduced dot space of $N-1$ sites $\mu=1, \dots, N-1$ are denoted by primed quantities. For such operators, the summation over sites μ starts from $\mu=1$ rather than $\mu=0$.

C. Site basis with good spin quantum numbers

The Hamiltonian \hat{H} in Eq. (8) is invariant under spin rotations and therefore conserves the total spin of the system (Kondo spin plus dot spin) $\hat{S}_{\text{tot}} = \hat{S}_K + \hat{S}_d = \hat{S}_{K0} + \hat{S}'_d$. To take advantage of this symmetry, it is convenient to use a basis for which both the total spin S_{tot} and the corresponding magnetic quantum number $M_{\text{tot}} \equiv S_{\text{tot}}^z$ are good quantum numbers.

There are different ways to construct a basis with good total spin but one of them is particularly useful in the strong-coupling limit $J_k \gg t_0, J_s$. To zeroth order in t_0/J_k and J_s/J_k , we can ignore the coupling term \hat{H}_{cp} , in which case the subsystem of Kondo spin plus site 0 decouples from the reduced dot. The Hamiltonian \hat{H}_{K0} is easily diagonalized by coupling the spins \hat{S}_K and \hat{s}_0 to $\hat{S}_{K0} \equiv \hat{S}_K + \hat{s}_0$, and using $\hat{S}_K \cdot \hat{s}_0 = (\hat{S}_{K0}^2 - \hat{S}_K^2 - \hat{s}_0^2)/2$. If site $\mu=0$ is singly occupied, i.e., $n_0=1$, this spin coupling will lead to either a singlet $S_{K0}=0$ (lowest energy) or a triplet $S_{K0}=1$ (highest energy). However, if site $\mu=0$ is empty ($n_0=0$) or doubly occupied ($n_0=2$), the spin at site 0 and the corresponding Kondo coupling term vanish.

This results in an unscreened Kondo spin in a doublet state ($S_{K0}=1/2$), the energy of which is intermediate between the singlet and triplet states.

We now construct a basis of good total spin that also reflects the division into singlet/doublet/triplet manifolds. The eigenstates of \hat{H}_{K0} are characterized by S_{K0}, M_{K0} with M_{K0} being the magnetic quantum number of \hat{S}_{K0} . The eigenstates of the reduced dot Hamiltonian \hat{H}'_d with $N-n_0$ electrons are characterized by $|\gamma' S'_d M'_d\rangle$, where S'_d, M'_d are the spin and spin projection, respectively, of the reduced dot and γ' denotes all other quantum numbers distinguishing between states with the same S'_d .³⁷ We then couple the above eigenstates of \hat{H}_{K0} with the eigenstates of the reduced dot to form states with good total spin and spin projection quantum numbers $S_{\text{tot}}, M_{\text{tot}}$. This basis of the coupled system is given by $|n_0, S_{K0}; \gamma', S'_d; S_{\text{tot}}, M_{\text{tot}}\rangle$. To keep the notation simple, we omitted the quantum numbers $S_K=1/2$ and $s_0=n_0(2-n_0)/2$.

Spin selection rules determine the allowed values of the reduced dot spin S'_d for a given value of the total spin S_{tot} . We have $S'_d = S_{\text{tot}}$ for the singlet subspace, $S'_d = S_{\text{tot}} \pm 1/2$ for the doublet subspace, and $S'_d = S_{\text{tot}}, S_{\text{tot}} \pm 1$ for the triplet subspace.

III. STRONG-COUPPLING HAMILTONIAN

The strong-coupling limit is defined by $J_k \gg t_0$. Since $t_0 \sim D \sim N\bar{\delta}$, this limit corresponds to $J_k \bar{\rho} \gg 1$, where $\bar{\rho} \approx 1/(N\bar{\delta})$ is the average single-particle level density per site.

In the strong-coupling limit, the lowest eigenstates of \hat{H} are dominated by the singlet manifold. The bare singlet Hamiltonian (in the limit when \hat{H}_{cp} is ignored) is given by the reduced dot Hamiltonian \hat{H}'_d with $N-1$ electrons (except for a constant shift). However, virtual transitions between the singlet and doublet/triplet manifolds add correction terms to this Hamiltonian. Our goal is to determine the resulting effective Hamiltonian of the reduced dot in the strong-coupling limit.

A. Projection technique

At finite Kondo interaction, the above three manifolds (singlet, doublet, and triplet) are coupled to each other. Specifically, the exchange term in \hat{H}_{cp} couples the singlet and triplet manifolds while the hopping term between sites 0 and 1 couples each of the singlet and triplet manifolds to the doublet manifold. To account for these couplings we define projection operators $\hat{P}_s/\hat{P}_d/\hat{P}_t$ on the corresponding singlet/doublet/triplet subspaces ($\hat{P}_s + \hat{P}_d + \hat{P}_t = 1$) and decompose the wave function $\psi = \psi_s + \psi_d + \psi_t$ accordingly.³⁸ The Schrödinger equation for the coupled system $\hat{H}\psi = E\psi$ can then be written as

$$\sum_{\beta=s,d,t} \hat{H}_{\alpha\beta} \psi_{\beta} = E \psi_{\alpha}, \quad (12)$$

where each of the two indices α, β assumes any of three values $\{s, d, t\}$ and $\hat{H}_{\alpha\beta} \equiv \hat{P}_{\alpha} \hat{H} \hat{P}_{\beta}$.

In the strong-coupling limit, our system is described to zeroth order by the singlet Hamiltonian \hat{H}_{ss} , which contains the bare reduced dot Hamiltonian \hat{H}'_d (for $N-1$ electrons) and \hat{H}_{K0} (which assumes a constant value), decoupled from each other. Higher-order corrections arise from the coupling terms in \hat{H}_{cp} which lead to an effective ‘‘dressed’’ Hamiltonian of the reduced dot. This effective Hamiltonian \hat{H}^{eff} is formally determined by eliminating ψ_d and ψ_t in Eq. (12) and by writing a single equation in the singlet manifold $\hat{H}^{\text{eff}}\psi_s = E\psi_s$, where \hat{H}^{eff} is given by

$$\begin{aligned} \hat{H}^{\text{eff}} &= \hat{H}_{ss} + \hat{H}'_{st}(E - \hat{H}_{tt})^{-1}\hat{H}_{ts} + [\hat{H}'_{sd} + \hat{H}'_{st}(E - \hat{H}_{tt})^{-1}\hat{H}'_{td}] \\ &\times \{E - [\hat{H}_{dd} + \hat{H}_{dt}(E - \hat{H}_{tt})^{-1}\hat{H}'_{td}]\}^{-1} \\ &\times [\hat{H}_{ds} + \hat{H}_{dt}(E - \hat{H}_{tt})^{-1}\hat{H}'_{ts}]. \end{aligned} \quad (13)$$

The diagonal components $\hat{H}_{\alpha\alpha}$ in the above equation are determined by evaluating \hat{H}_{K0} [Eq. (9)] in each of the three subspaces $\alpha = \{s, d, t\}$. The coupling terms in \hat{H}_{cp} [Eq. (11)] do not contribute to these diagonal components with the exception of $\hat{s}_0 \cdot \hat{S}'_d$ which contributes to \hat{H}_{tt} only. We find

$$\hat{H}_{ss} = \hat{P}_s \left(\varepsilon_0^c - \frac{3J_k}{4} - \frac{3J_s}{4} + \hat{H}'_d \right) \hat{P}_s, \quad (14)$$

$$\hat{H}_{dd} = \hat{P}_d (\varepsilon_0^c \hat{n}_0 + \hat{H}'_d) \hat{P}_d, \quad (15)$$

$$\hat{H}_{tt} = \hat{P}_t \left(\varepsilon_0^c + \frac{J_k}{4} - \frac{3J_s}{4} + \hat{H}'_d - 2J_s \hat{s}_0 \cdot \hat{S}'_d \right) \hat{P}_t. \quad (16)$$

Contributions to off-diagonal components $\hat{H}_{\alpha\beta}$ with $\alpha \neq \beta$ originate in \hat{H}_{cp} . The hopping term in \hat{H}_{cp} changes the spin S_{K0} by $\pm 1/2$ and can only couple the doublet to each of the singlet and triplet manifolds while the exchange term $\hat{s}_0 \cdot \hat{S}'_d$ in \hat{H}_{cp} only couples the singlet and triplet manifolds.

B. Expansion in the strong-coupling limit

The above effective Hamiltonian \hat{H}^{eff} and the construction of a good spin basis are exact, in that no approximations were made beyond the original Hamiltonian \hat{H} in Eq. (2). However, the form (13) of \hat{H}^{eff} is not very useful for practical calculations. In the strong-coupling limit, $J_k \gg t_0 \sim N\bar{\delta}$, we can expand \hat{H}^{eff} in the two small dimensionless parameters $t_0/J_k \sim 1/(J_k\bar{\rho})$ and J_s/J_k .³⁹ We will do so up to fourth order in these parameters, where the expansion terms are measured in units of J_k (this energy unit is set by the energy of the singlet).

The starting point for this expansion is the unperturbed singlet Hamiltonian \hat{H}_{ss} , the eigenbasis of which is given by $|n_0=1, S_{K0}=0; \gamma', S'_d; S_{\text{tot}}=S'_d, M_{\text{tot}}\rangle$. The corresponding eigenvalues are

$$E_m^{(0)} = -\frac{3}{4}(J_k + J_s) + \varepsilon_0^c + E'_{0,m} - J_s S_{\text{tot}}(S_{\text{tot}} + 1), \quad (17)$$

where $E'_{0,m}$ are the eigenvalues of \hat{H}'_0 . These unperturbed eigenvalues, $E_m^{(0)}$, are the limiting solutions to which the eigenvalues E_m of the full Hamiltonian in Eq. (13) converge in the limit $J_k \rightarrow \infty$. The differences between $E_m^{(0)}$ and E_m at large but finite values of J_k are induced by the virtual transitions from the singlet to the doublet or triplet subspaces. These virtual excitations, in turn, give rise to effective interaction terms in the reduced dot, denoted by $\delta\hat{H}^{\text{eff}}$. The full effective Hamiltonian in the singlet manifold is then given by $\hat{H}^{\text{eff}} = \hat{H}_{ss} + \delta\hat{H}^{\text{eff}}$.

The effective interaction terms in $\delta\hat{H}^{\text{eff}}$ must be consistent with charge and spin conservation.² In particular, $\delta\hat{H}^{\text{eff}}$ must be a scalar operator in spin space (i.e., invariant under rotations in spin space) and invariant under time reversal. This restricts the possible terms that appear in the effective Hamiltonian.

Scalar one-body terms, i.e., \hat{n}_1 and $(\sum_{\sigma} \hat{c}_{1,\sigma}^\dagger \hat{c}_{2,\sigma} + \text{H.c.})$ lead to a renormalization of the one-body part of the reduced dot Hamiltonian \hat{H}'_d . Two-body scalars that can be constructed from the spin \hat{S}'_1 at site 1 and the total spin of the reduced dot \hat{S}'_d are \hat{s}_1^2 , $\hat{s}_1 \cdot \hat{S}'_d$, and $\hat{S}'_d{}^2$. The first, $\hat{s}_1^2 = \frac{3}{4}\hat{n}_1(2 - \hat{n}_1)$ is the Nozières term known from the conventional Kondo problem³⁶ in the absence of exchange ($J_s=0$) but the other two terms are new. The scalar triple product $i\hat{S}'_d \cdot (\hat{s}_1 \times \hat{S}'_d)$ (the imaginary i is necessary for time-reversal invariance) does not lead to an additional term since $i\hat{S}'_d \cdot (\hat{s}_1 \times \hat{S}'_d) = -\hat{s}_1 \cdot \hat{S}'_d$ while a fourth-order invariant is given by $\hat{S}'_d{}^4$. Other invariants such as $\hat{S}'_d \cdot \sum_{\sigma,\sigma'} (\hat{c}_{1,\sigma}^\dagger \tau_{\sigma,\sigma'} \hat{c}_{2,\sigma'}) + \text{H.c.}$, $\hat{S}'_d \cdot \sum_{\sigma,\sigma'} (\hat{c}_{2,\sigma}^\dagger \tau_{\sigma,\sigma'} \hat{c}_{1,\sigma'}) + \text{H.c.}$, and $\hat{s}_1 \cdot \hat{S}'_d \sum_{\sigma} (\hat{c}_{1,\sigma}^\dagger \hat{c}_{2,\sigma} + \hat{c}_{2,\sigma}^\dagger \hat{c}_{1,\sigma}) + \text{H.c.}$ are allowed but, as we shall see, they cancel out in \hat{H}^{eff} .

We rewrite the effective Hamiltonian in Eq. (13) as $\hat{H}^{\text{eff}} = \hat{H}_{ss} + \sum_{i=1}^4 \delta\hat{H}_i$, where

$$\delta\hat{H}_1 = \hat{H}_{sd} \frac{1}{(E - \hat{H}_{dd}) + \hat{H}_{dt} \frac{1}{E - \hat{H}_{tt}} \hat{H}'_{td}} \hat{H}_{ds},$$

$$\delta\hat{H}_2 = \hat{H}_{st} \frac{1}{E - \hat{H}_{tt}} \hat{H}_{ts},$$

$$\delta\hat{H}_3 \approx \hat{H}_{st} \frac{1}{E - \hat{H}_{tt}} \hat{H}'_{td} \frac{1}{E - \hat{H}_{dd}} \hat{H}_{ds} + \text{H.c.},$$

$$\delta\hat{H}_4 \approx \hat{H}_{st} \frac{1}{E - \hat{H}_{tt}} \hat{H}'_{td} \frac{1}{E - \hat{H}_{dd}} \hat{H}_{dt} \frac{1}{E - \hat{H}_{tt}} \hat{H}_{ts}. \quad (18)$$

In the terms $\delta\hat{H}_3$ and $\delta\hat{H}_4$ above we have replaced $\hat{H}_{dd} + \hat{H}_{dt}(E - \hat{H}_{tt})^{-1}\hat{H}'_{td}$ by \hat{H}_{dd} (the neglected term gives contributions that are higher than fourth order in the expansion parameters).

We next expand each $\delta\hat{H}_i$ to fourth order in the parameters t_0/J_k and J_s/J_k . Since the energy E is of the order J_k , the fractions appearing in each term can be brought to a form $1/(1-\hat{X})$ with \hat{X} being small in the expansion parameters. We then approximate $1/(1-\hat{X}) \approx 1+\hat{X}+\hat{X}^2$. In the following we summarize the explicit calculation of each term.

1. Evaluation of $\delta\hat{H}_1$

For $\delta\hat{H}_1$ we find

$$\delta\hat{H}_1 \approx -\frac{4}{3J_k}\hat{H}_{sd}(1+\hat{A}+\hat{B}+\hat{C}+\hat{A}^2+\hat{B}^2)\hat{H}_{ds}, \quad (19)$$

where

$$\hat{A} = \frac{4}{3J_k}[E'_0 - \hat{H}'_0 + \varepsilon_0^c(1 - \hat{n}_0)], \quad (20)$$

$$\hat{B} = \frac{4}{3J_k}J_s[-3/4 - S_{\text{tot}}(S_{\text{tot}} + 1) + \hat{\mathbf{S}}_d'^2], \quad (21)$$

$$\hat{C} = \frac{4}{3J_k^2}\hat{H}_{sd}\hat{H}_{ds}. \quad (22)$$

In Eq. (19), we omitted the product terms $\hat{A}\hat{C}$, $\hat{B}\hat{C}$, \hat{C}^2 since their contribution is higher than fourth order, while the contribution of $\hat{A}\hat{B}+\hat{B}\hat{A}$ can be shown to vanish identically.

To keep track of the various contributions for each of the $\delta\hat{H}_i$, we label them in the following by $\delta\hat{H}_{i,j}$. These terms are understood to act only in the space of the reduced dot while the Kondo spin and the spin on site 0 are locked into a singlet. The operators $\delta\hat{H}_{i,j}$ in the reduced dot space are obtained by taking a partial expectation value $\langle \dots \rangle_s$ in the singlet state. The corresponding operators in the full space are given, respectively, by $P_s \langle \dots \rangle_s P_s$. In the Appendix we list several relations that are useful in calculating the expectation values of various operators in the singlet space.

The most dominant contribution to Eq. (19) arises from the unity operator term (in the round brackets). We find

$$\delta\hat{H}_{1,1} \equiv -\frac{4}{3J_k}\langle \hat{H}_{sd}\hat{H}_{ds} \rangle_s = -\frac{4}{3J_k}\langle \hat{H}_{\text{hop}}^{(0,1)}\hat{H}_{\text{hop}}^{(0,1)} \rangle_s = -\frac{4}{3J_k}|t_0|^2, \quad (23)$$

where we have substituted \hat{H}_{sd} by the hopping Hamiltonian between sites 0 and 1,

$$\hat{H}_{\text{hop}}^{(0,1)} = \sum_{\sigma} t_0 \hat{c}_{0,\sigma}^{\dagger} \hat{c}_{1,\sigma} + \text{H.c.}, \quad (24)$$

and used Eq. (A7). Alternatively, $\hat{H}_{sd}\hat{H}_{ds}$ describes the spin transitions illustrated in Fig. 2(a), and the result in Eq. (23) can be derived using Table I in the Appendix to sum up all the corresponding transition pathways.

The term containing \hat{A} in Eq. (19) yields corrections that are second order in t_0/J_k . Using the difference in the values of \hat{H}'_0 , \hat{n}_0 in the singlet and doublet subspaces, and Eqs. (A11) and (A12), we find

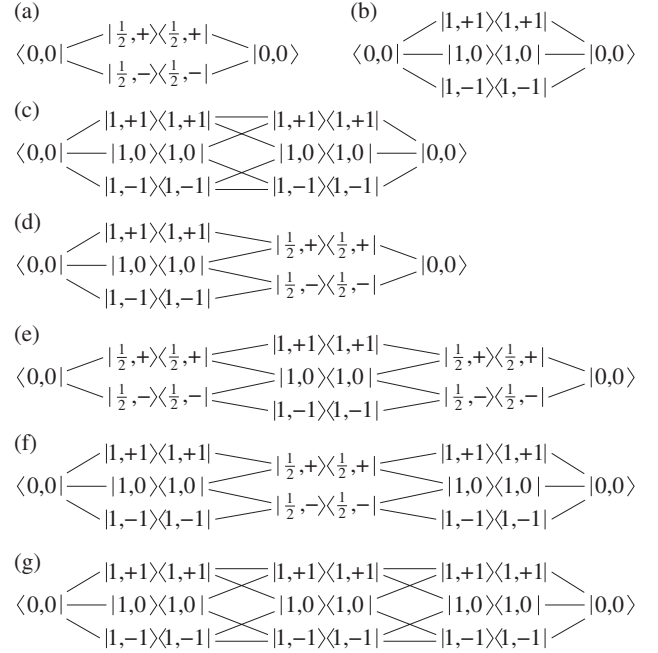


FIG. 2. Spin-transition diagrams used to derive the effective strong-coupling Hamiltonian in Eq. (53). All transitions connect two singlet states, characterized by the quantum numbers $S_{K0} = 0$, $S_{K0,z} = 0$. The intermediate transition pathways involve combinations of doublet ($S_{K0} = 1/2$, $S_{K0,z} = \pm 1/2$) and triplet ($S_{K0} = 1$, $S_{K0,z} = \pm 1, 0$) states.

$$\delta\hat{H}_{1,2} \equiv -\frac{4}{3J_k}\langle \hat{H}_{sd}\hat{A}\hat{H}_{ds} \rangle_s = -\left(\frac{4}{3J_k}\right)^2|t_0|^2\left[(\varepsilon_0^c - \varepsilon_1^c) + (\varepsilon_1^c - \varepsilon_0^c)\hat{n}_1 + \frac{1}{2}\sum_{\sigma} (t_1\hat{c}_{1\sigma}^{\dagger}\hat{c}_{2\sigma} + \text{H.c.})\right]. \quad (25)$$

The constant shift in Eq. (25) can be incorporated into \hat{H}_{ss} in Eq. (14) by redefining ε_0^c , while the one-body operator in Eq. (25) can be incorporated into the Hamiltonian \hat{H}'_0 by redefining the site energy ε_1^c and the hopping amplitude t_1 .³⁸

$$\varepsilon_0^c \rightarrow \varepsilon_0^c - \left(\frac{4|t_0|}{3J_k}\right)^2(\varepsilon_0^c - \varepsilon_1^c),$$

$$\varepsilon_1^c \rightarrow \varepsilon_1^c - \left(\frac{4|t_0|}{3J_k}\right)^2(\varepsilon_1^c - \varepsilon_0^c), \quad (26)$$

$$t_1 \rightarrow t_1 \left[1 - \frac{1}{2}\left(\frac{4|t_0|}{3J_k}\right)^2\right]. \quad (27)$$

The term involving \hat{B} in Eq. (19) contributes only for a finite exchange interaction ($J_s \neq 0$). We have

$$\langle \hat{H}_{sd}\hat{\mathbf{S}}_d'^2\hat{H}_{ds} \rangle_s = \frac{|t_0|^2}{2}\sum_{\sigma} (\hat{c}_{1\sigma}^{\dagger}\hat{\mathbf{S}}_d'^2\hat{c}_{1\sigma} + \hat{c}_{1\sigma}\hat{\mathbf{S}}_d'^2\hat{c}_{1\sigma}^{\dagger}). \quad (28)$$

Using the identities (A5) and (A6), Eq. (28) can be simplified to give Eq. (A15) in the Appendix. Using $S'_d = S_{\text{tot}}$ in the singlet subspace, we obtain

$$\delta\hat{H}_{1,3} \equiv -\frac{4}{3J_k} \langle \hat{H}_{sd} \hat{B} \hat{H}_{ds} \rangle_s = 2J_s \left(\frac{4|t_0|}{3J_k} \right)^2 \hat{s}_1 \cdot \hat{S}'_d. \quad (29)$$

We note that $\delta\hat{H}_{1,3}$ is a spin invariant in the reduced dot space.

The term involving \hat{C} in Eq. (19) is given by

$$\delta\hat{H}_{1,4} \equiv -\frac{16}{9J_k^3} \langle \hat{H}_{sd} \hat{H}_{dt} \hat{H}_{td} \hat{H}_{ds} \rangle_s. \quad (30)$$

This term appears in the conventional Kondo problem (where $J_s=0$) and is known as the Nozières term. Nozières³⁶ found that this term yields an effective interaction in the singlet space that repels opposite spins on site 1. This term is induced by virtual transitions of the type singlet-doublet-triplet-doublet-singlet. Once we insert a triplet projection \hat{P}_t in the rhs of Eq. (30), i.e., we write the corresponding singlet expectation value as $\langle \hat{H}_{sd} \hat{H}_{dt} \hat{P}_t \hat{H}_{td} \hat{H}_{ds} \rangle_s$, we can replace both \hat{H}_{sd} and \hat{H}_{dt} by the hopping Hamiltonian $\hat{H}_{\text{hop}}^{(0,1)}$ between sites 0 and 1 [see Eq. (24)]. Using $\hat{H}_{\text{hop}}^{(0,1)} \hat{P}_t \hat{H}_{\text{hop}}^{(0,1)} = \hat{H}_{\text{hop}}^{(0,1)} \hat{H}_{\text{hop}}^{(0,1)} - \hat{H}_{\text{hop}}^{(0,1)} \hat{P}_s \hat{H}_{\text{hop}}^{(0,1)}$, we have

$$\langle \hat{H}_{sd} \hat{H}_{dt} \hat{H}_{td} \hat{H}_{ds} \rangle_s = \langle \hat{H}_{\text{hop}}^{(0,1)} \hat{H}_{\text{hop}}^{(0,1)} \hat{H}_{\text{hop}}^{(0,1)} \hat{H}_{\text{hop}}^{(0,1)} \rangle_s - |\langle \hat{H}_{\text{hop}}^{(0,1)} \hat{H}_{\text{hop}}^{(0,1)} \rangle_s|^2. \quad (31)$$

With the help of Eqs. (A1), (A2), (A7), and (A11), we then find

$$\delta\hat{H}_{1,4} = -3 \left(\frac{4}{3J_k} \right)^3 |t_0|^4 \hat{s}_1^2 = -\frac{16}{3J_k^3} |t_0|^4 \hat{n}_1 (2 - \hat{n}_1). \quad (32)$$

An alternative way to calculate $\delta\hat{H}_{1,4}$ is to use the spin diagram in Fig. 2(e). It can be reduced to the transition diagram in Fig. 2(b) with the help of Table I in the Appendix.

The Nozières term (32) vanishes when site 1 is either empty ($n_1=0$) or doubly occupied ($n_1=2$) but is negative for $n_1=1$, thus favoring a singly occupied site 1.

The contribution from \hat{A}^2 in Eq. (19) is evaluated using Eqs. (A13) and (A14) and leads to a constant shift

$$\begin{aligned} \delta\hat{H}_{1,5} &\equiv -\frac{4}{3J_k} \langle \hat{H}_{sd} \hat{A}^2 \hat{H}_{ds} \rangle_s \\ &= -\left(\frac{4}{3J_k} \right)^3 |t_0|^2 [|t_1|^2 + (\varepsilon_0^c)^2 + (\varepsilon_1^c)^2 - 2\varepsilon_0^c \varepsilon_1^c]. \end{aligned} \quad (33)$$

Finally, the contribution from \hat{B}^2 in Eq. (19) is found to be

$$\delta\hat{H}_{1,6} \equiv -\left(\frac{4}{3J_k} \right)^3 |t_0|^2 J_s^2 (\hat{S}'_d{}^2 + 2\hat{s}_1 \cdot \hat{S}'_d), \quad (34)$$

where we have used Eq. (A16).

2. Evaluation of $\delta\hat{H}_2$

We next turn to the singlet-triplet transitions as described by $\delta\hat{H}_2$ in Eq. (18). The corresponding expression for $\delta\hat{H}_2$ is given by

$$\delta\hat{H}_2 \approx -\frac{1}{J_k} \hat{H}_{st} (1 + \hat{D} + \hat{E} + \hat{E}^2) \hat{H}_{ts}, \quad (35)$$

where

$$\hat{D} = \frac{1}{J_k} [E'_0 - \hat{H}'_0], \quad (36)$$

$$\hat{E} = \frac{J_s}{J_k} [-S_{\text{tot}}(S_{\text{tot}} + 1) + \hat{S}'_d{}^2 + 2\hat{s}_0 \cdot \hat{S}'_d]. \quad (37)$$

In Eq. (35) we omitted the terms \hat{D}^2 and $\hat{D}\hat{E}$, which can be shown to vanish.

The dominating term in Eq. (35) is the one involving the unity operator. The corresponding term induces a spin transition as in Fig. 2(b). Using $\hat{H}_{st} = -2J_s \hat{P}_s (\hat{s}_0 \cdot \hat{S}'_d) \hat{P}_t$ and Eq. (A9) we find

$$\delta\hat{H}_{2,1} \equiv -\frac{1}{J_k} \langle \hat{H}_{st} \hat{H}_{ts} \rangle_s = -\frac{J_s^2}{J_k} \hat{S}'_d{}^2. \quad (38)$$

The same result can also be obtained with the help of Table II in the Appendix. The contribution $\delta\hat{H}_{2,2}$ induced by the term involving \hat{D} in Eq. (35) can be simplified using $\langle \hat{H}_{st} \hat{H}'_0 \hat{H}_{ts} \rangle_s = J_s^2 \hat{S}'_d \hat{H}'_0 \hat{S}'_d$. Since \hat{S}'_d commutes with the scalar operator \hat{H}'_0 , we find

$$\delta\hat{H}_{2,2} \equiv -\frac{1}{J_k} \langle \hat{H}_{st} \hat{D} \hat{H}_{ts} \rangle_s = 0. \quad (39)$$

The contribution $\delta\hat{H}_{2,3}$ induced by the term \hat{E} in Eq. (35) can also be simplified since $\hat{S}'_d{}^2$ acts in the reduced dot space (and therefore has identical action in the singlet and triplet manifolds). The resulting expression gives rise to transition pathways as shown in Fig. 2(c), the sum over which is further simplified using Eq. (A10) to give

$$\delta\hat{H}_{2,3} \equiv -\frac{1}{J_k} \langle \hat{H}_{st} \hat{E} \hat{H}_{ts} \rangle_s = \frac{J_s^3}{J_k^2} \hat{S}'_d{}^2. \quad (40)$$

The last term $\delta\hat{H}_{2,4}$ in Eq. (35), containing \hat{E}^2 , is found to be $\delta\hat{H}_{2,4} = -(16J_s^4/J_k^3) (\hat{s}_0 \cdot \hat{S}'_d)^4$ and corresponds to the transition diagram in Fig. 2(g). Since \hat{H}_{st} (a scalar operator) commutes with $\hat{S}'_d{}^2$, all other terms vanish identically. Using Eq. (A3) this expression can be simplified to give

$$\delta\hat{H}_{2,4} \equiv -\frac{1}{J_k} \langle \hat{H}_{st} \hat{E}^2 \hat{H}_{ts} \rangle_s = -\frac{J_s^4}{J_k^3} \hat{S}'_d{}^2. \quad (41)$$

3. Evaluation of $\delta\hat{H}_3$

Following Eq. (18), the subsequent contribution, $\delta\hat{H}_3$, involves transitions to both the doublet and the triplet subspaces

$$\delta\hat{H}_3 \approx \frac{4}{3J_k^2} \hat{H}_{st}(1 + \hat{D} + \hat{E})\hat{H}_{td}(1 + \hat{A} + \hat{B})\hat{H}_{ds} + \text{H.c.}, \quad (42)$$

where the operators $\hat{A}-\hat{E}$ are the same as introduced above. Contributions involving products between \hat{D}, \hat{E} and \hat{A}, \hat{B} are higher than fourth order in the expansion parameters and are therefore not considered here.

The dominant contribution, $\delta\hat{H}_{3,1}$ originates in the transitions shown in Fig. 2(d). Using Table I we can simplify this transition diagram to the one of Fig. 2(b), for which we obtain

$$\delta\hat{H}_{3,1} \equiv \frac{4}{3J_k^2} \langle \hat{H}_{st}\hat{H}_{td}\hat{H}_{ds} \rangle_s + \text{H.c.} = \frac{16J_s}{3J_k^2} |t_0|^2 \hat{\mathbf{s}}_1 \cdot \hat{\mathbf{S}}'_d. \quad (43)$$

To simplify the term $\delta\hat{H}_{3,2}$, involving \hat{D} in Eq. (42), we make use of $[\hat{H}_{st}, \hat{H}'_0]=0$ and find

$$\begin{aligned} \delta\hat{H}_{3,2} &\equiv \frac{4}{3J_k^2} \hat{H}_{st}\hat{D}\hat{H}_{td}\hat{H}_{ds} + \text{H.c.} \\ &= \frac{8J_s}{3J_k^3} |t_0|^2 (E'_0 - \hat{H}'_0) \hat{\mathbf{s}}_1 \cdot \hat{\mathbf{S}}'_d + \text{H.c.} \end{aligned} \quad (44)$$

The diagonal matrix elements of $\delta\hat{H}_{3,2}$ (when evaluated in the eigenstates of the reduced dot) vanish. Off-diagonal matrix elements enter in second-order perturbation theory (for the effective Hamiltonian) and would lead to a correction $\sim J_s^2 |t_0|^4 / J_k^6$ that is beyond the fourth-order approximation. A convenient choice for E'_0 is its average energy in the two reduced dot eigenstates (appearing in the corresponding matrix element). This choice leads to

$$\delta\hat{H}_{3,2} = 0. \quad (45)$$

The next term $\delta\hat{H}_{3,3}$, produced by \hat{E} in Eq. (42), can be calculated using Table I and the diagram in Fig. 2(c), where a sum of all relevant terms can be identified with Eq. (A4), yielding

$$\delta\hat{H}_{3,3} \equiv \frac{4}{3J_k^2} \langle \hat{H}_{st}\hat{E}\hat{H}_{td}\hat{H}_{ds} \rangle_s + \text{H.c.} = -\frac{8J_s^2}{3J_k^3} |t_0|^2 \hat{\mathbf{s}}_1 \cdot \hat{\mathbf{S}}'_d + \text{H.c.} \quad (46)$$

The contribution $\delta\hat{H}_{3,4}$ induced by \hat{A} in Eq. (42), is calculated to be

$$\begin{aligned} \delta\hat{H}_{3,4} &\equiv \frac{4}{3J_k^2} \langle \hat{H}_{st}\hat{H}_{td}\hat{A}\hat{H}_{ds} \rangle_s + \text{H.c.} \\ &= \frac{32J_s}{9J_k^3} |t_0|^2 \hat{\mathbf{s}}_1 \cdot \hat{\mathbf{S}}'_d (E'^{(0)} - \hat{H}'_0) + \text{H.c.} \end{aligned} \quad (47)$$

Following the same arguments used for the evaluation of $\delta\hat{H}_{3,2}$, we find $\delta\hat{H}_{3,4}=0$.

The term \hat{B} in Eq. (42) gives rise to a transition diagram of the type shown in Fig. 2(d) which can be reduced to a diagram as in Fig. 2(b) with the help of Table III. Further

simplifications involving several of the equations in the Appendix yield

$$\begin{aligned} \delta\hat{H}_{3,5} &\equiv \frac{4}{3J_k^2} \langle \hat{H}_{st}\hat{H}_{td}\hat{B}\hat{H}_{ds} \rangle_s + \text{H.c.} \\ &= -\frac{J_s^2}{J_k} \left(\frac{4}{3J_k} \right)^2 |t_0|^2 (\hat{\mathbf{S}}_d'^2 + 2\hat{\mathbf{s}}_1 \cdot \hat{\mathbf{S}}'_d) + \text{H.c.} \end{aligned} \quad (48)$$

4. Evaluation of $\delta\hat{H}_4$

To determine the terms contributing to $\delta\hat{H}_4$ (up to fourth order), we make the following approximations in Eq. (18): $(E - \hat{H}_{tt})^{-1} \approx -1/J_k$ and $(E - \hat{H}_{dd})^{-1} \approx -4/(3J_k)$. The resulting expression for $\delta\hat{H}_4$ corresponds to a transition diagram as in Fig. 2(f). Using Eqs. (A1), (A4), (A9), and (A10) we find

$$\delta\hat{H}_4 \approx -\frac{4}{3J_k^3} \langle \hat{H}_{st}\hat{H}_{td}\hat{H}_{dt}\hat{H}_{ts} \rangle = -\frac{4J_s^2}{3J_k^3} |t_0|^2 (\hat{\mathbf{S}}_d'^2 + 2\hat{\mathbf{s}}_1 \cdot \hat{\mathbf{S}}'_d). \quad (49)$$

Alternatively, we can obtain this result using Table I to get a transition diagram as in Fig. 2(c), which can then be simplified using Eq. (A4).

5. Additional terms

In the above calculations, we have replaced the energy eigenvalue E in Eq. (13) by its unperturbed value $E^{(0)}$ in Eq. (17). However, additional terms to the effective Hamiltonian are found when corrections to $E^{(0)}$ are included self-consistently. To the order we are interested in, it is sufficient to consider $\delta\hat{H}_{1,1}$ and $\delta\hat{H}_{2,1}$ [see Eqs. (23) and (38), respectively] as corrections to $E^{(0)}$

$$E \approx E^{(0)} - \frac{4|t_0|^2}{3J_k} - \frac{J_s^2}{J_k} S_{\text{tot}}(S_{\text{tot}} + 1). \quad (50)$$

Adding these correction terms inside the square brackets in Eq. (20) gives the following term

$$\delta\hat{H}_{1,7} \equiv \left(\frac{4}{3J_k} \right)^3 |t_0|^4 + \left(\frac{4J_s}{3J_k} \right)^2 \frac{|t_0|^2}{J_k} \hat{\mathbf{S}}_d'^2. \quad (51)$$

A similar correction inside the square brackets of Eq. (36) yields

$$\delta\hat{H}_{2,5} \equiv \frac{4J_s^2}{3J_k^3} |t_0|^2 \hat{\mathbf{S}}_d'^2 + \frac{J_s^4}{J_k^3} \hat{\mathbf{S}}_d'^4. \quad (52)$$

Up to fourth order, the corrections from Eq. (50) do not lead to additional terms in $\delta\hat{H}_3$ and $\delta\hat{H}_4$.

C. Effective Hamiltonian: A complete expression

Collecting all the terms found in the previous section, the effective Hamiltonian $\hat{H}^{\text{eff}} = \hat{H}_{ss} + \sum_{i=1}^4 \delta\hat{H}_i$ is given (to fourth order in t_0/J_k and J_s/J_k) by

$$\begin{aligned} \hat{H}^{\text{eff}} \approx & \eta + \tilde{H}'_d - \left(\frac{4}{3J_k}\right)^3 |t_0|^4 (3\hat{S}_1^2 - 1) \\ & + J_k \left(\frac{80J_s}{9J_k} - \frac{536J_s^2}{27J_k^2}\right) \frac{|t_0|^2}{J_k^2} \hat{S}_1 \cdot \hat{S}'_d + \frac{J_s^4}{J_k^3} \hat{S}'_d{}^4, \end{aligned} \quad (53)$$

where η is a constant

$$\begin{aligned} \eta = & \varepsilon_0^c - \frac{3(J_k + J_s)}{4} - \frac{4|t_0|^2}{3J_k} - \left(\frac{4|t_0|}{3J_k}\right)^2 (\varepsilon_0^c - \varepsilon_1^c) \\ & - \left(\frac{4}{3J_k}\right)^3 |t_0|^2 [|t_1|^2 + (\varepsilon_0^c)^2 + (\varepsilon_1^c)^2 - 2\varepsilon_0^c \varepsilon_1^c], \end{aligned} \quad (54)$$

and \tilde{H}'_d describes a renormalized universal Hamiltonian for the reduced dot

$$\tilde{H}'_d = \tilde{H}'_0 - \tilde{J}_s \hat{S}'_d{}^2. \quad (55)$$

\tilde{H}'_0 is a renormalized one-body Hamiltonian of the reduced dot, obtained from \hat{H}'_0 by redefining ε_1^c and t_1 according to Eqs. (26) and (27), respectively. This tridiagonal Hamiltonian can be rediagonalized $\tilde{H}'_0 = \sum_{n=1}^{N-1} \sigma \tilde{\varepsilon}_n^\sigma \hat{a}_{n\sigma}^\dagger \hat{a}_{n\sigma}$ to define new effective single-particle orbitals $\hat{a}_{n\sigma}^\dagger |0\rangle$ and energies $\tilde{\varepsilon}_n^\sigma$ of the reduced dot. \tilde{J}_s in Eq. (55) is a renormalized exchange constant

$$\tilde{J}_s = J_s \left(1 + \frac{J_s}{J_k} - \frac{J_s^2}{J_k^2} + \frac{J_s^3}{J_k^3} + \frac{112J_s|t_0|^2}{27J_k^3} \right). \quad (56)$$

The most dominant contributions in Eq. (56) are positive and thus lead to a stronger exchange interaction in the reduced dot than in the original dot, $\tilde{J}_s > J_s$. Since the Kondo spin and the spin at site 0 are coupled to a singlet, the spin of the reduced dot $\hat{S}'_d = \hat{S}_{\text{tot}}$, and is thus conserved (i.e., $S'_d = S_{\text{tot}}$ and $M'_d \equiv S'_{d,z} = M_{\text{tot}}$ are good quantum numbers).

The effective Hamiltonian of the reduced dot contains several additional interaction terms, see Eq. (53). The term proportional to $(3\hat{S}_1^2 - 1)$ is the Nozières term, known from the conventional Kondo problem in the absence of exchange ($J_s = 0$).³⁶ The term proportional to $\hat{S}_1 \cdot \hat{S}'_d$ is an effective interaction in the reduced dot that is induced by the finite exchange interaction ($J_s \neq 0$) and describes an exchange interaction between the spin at site 1 and the spin of the reduced dot. This exchange interaction is to leading-order antiferromagnetic but depending on the particular values of J_k and J_s it can become ferromagnetic. The last term in Eq. (53) is a four-body term but it can be easily evaluated in terms of the conserved total spin S_{tot} (since $\hat{S}'_d = \hat{S}_{\text{tot}}$ in the singlet space). It can be combined with the renormalized exchange interaction in the reduced dot by defining an exchange coupling that depends on the total spin.

IV. EIGENVALUES OF THE EFFECTIVE HAMILTONIAN

The effective Hamiltonian of the reduced dot is valid to fourth order in t_0/J_k and J_s/J_k (when its terms are measured in units of J_k). To determine its eigenenergies to this fourth

order, it is sufficient to solve \hat{H}^{eff} in *first-order* perturbation theory. Both \tilde{H}'_d and $\hat{S}'_d{}^4$ are diagonal in a basis of good orbital occupations and good total spin of the reduced dot while a second-order perturbation theory of the remaining interaction terms leads to terms that are higher than fourth order in the combined power of t_0/J_k and J_s/J_k .

As required by first-order perturbation theory, we evaluate the expectation value of \hat{H}^{eff} in the unperturbed basis, i.e., in the eigenbasis of the renormalized universal Hamiltonian \tilde{H}'_d of the reduced dot. For simplicity, we will denote the good spin eigenstates of \tilde{H}'_d by $|\xi\rangle$ and the corresponding expectation values by $\langle \dots \rangle_\xi$.

The calculation of $\langle \hat{S}_1^2 \rangle_\xi$ in Eq. (53) simplifies for the lowest eigenstate of \tilde{H}'_d at each given spin value $S'_d = S_{\text{tot}}$. Those eigenstates of \tilde{H}'_d with $M'_d = S'_d$ have a maximal spin projection with only spin-up electrons in singly occupied levels and thus have $\hat{n}_{\bar{n}\sigma}$ as good quantum numbers (in contrast to a general eigenstate of \tilde{H}'_d , where only the orbital occupation numbers $\hat{n}_{\bar{n}}$ are well defined). For these states we have

$$\langle \hat{S}_1^2 \rangle_\xi = \frac{3}{4} \sum_{\sigma=\pm} \langle \hat{n}_{1\sigma} (1 - \hat{n}_{1-\sigma}) \rangle_\xi = \frac{3}{4} \sum_{\sigma=\pm} \langle \hat{n}_{1\sigma} \rangle_\xi (1 - \langle \hat{n}_{1-\sigma} \rangle_\xi). \quad (57)$$

The occupation $\langle \hat{n}_{1\sigma} \rangle_\xi$ can be calculated from $\langle \hat{n}_{1\sigma} \rangle_\xi = \sum_{\bar{n}=1}^{N-1} |U'_{1\bar{n}}|^2 \langle \hat{n}_{\bar{n}\sigma} \rangle_\xi$, where U' is the unitary matrix (of order $N-1$) transforming between the renormalized single-particle orbitals of the reduced dot (with creation operators $\hat{a}_{\bar{n}\sigma}^\dagger$) and the site basis states $\mu = 1, \dots, N-1$

$$\hat{c}_{\mu,\sigma}^\dagger = \sum_{\bar{n}=1}^{N-1} U'_{\mu,\bar{n}} \hat{a}_{\bar{n},\sigma}^\dagger. \quad (58)$$

For the good spin eigenstates of \tilde{H}'_d with $M'_d = S'_d$, the expectation value of $\hat{S}_1 \cdot \hat{S}'_d$ is given by

$$\begin{aligned} \langle \hat{S}_1 \cdot \hat{S}'_d \rangle_\xi &= (1 + S'_d) \langle \hat{s}_{1,z} \rangle_\xi = \frac{1 + S'_d}{2} \sum_{\sigma=\pm} \sigma \langle \hat{c}_{1\sigma}^\dagger \hat{c}_{1\sigma} \rangle_\xi \\ &= \frac{1 + S'_d}{2} \sum_{\sigma=\pm} \sum_{\bar{n}=1}^{N-1} \sigma |U'_{1\bar{n}}|^2 \langle \hat{n}_{\bar{n}\sigma} \rangle_\xi. \end{aligned} \quad (59)$$

Using Eqs. (57) and (59), we can calculate the lowest many-body eigenenergy for each total spin value of the Kondo Hamiltonian (2) up to fourth order in t_0/J_k and J_s/J_k .

V. COMPARISON WITH EXACT NUMERICAL DIAGONALIZATION

To validate our expression (53) for the effective Hamiltonian, we compare our analytical results for the many-body energies in the strong-coupling limit with an exact numerical diagonalization of the Hamiltonian (2) in a good spin basis scheme we developed previously.^{27,37}

As a first test, we compare results for the lowest energy of a given total spin (e.g., $S_{\text{tot}} = 3$). In Fig. 3, we show the difference ΔE (in units of J_k) between the energy determined

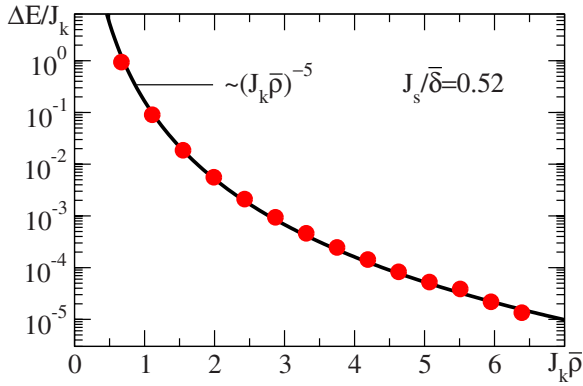


FIG. 3. (Color online) Energy difference ΔE (in units of J_k) between the estimate based on the effective Hamiltonian (53) and the exact numerical result for the lowest energy in the subspace $S_{\text{tot}}=3$. The quantum dot contains 11 electrons in 11 spin-degenerate single-particle energy levels ε_n^0 chosen from an arbitrary random matrix realization but with nonfluctuating orbital wave functions $\phi_n(0)=1/\sqrt{N}$. The results, shown for an arbitrary but fixed value $J_s/\bar{\delta}=0.52$ (red dots), behave like $\sim 1/(J_k\bar{\rho})^5$ (black solid line), expected for a strong-coupling expansion up to fourth order in $1/(J_k\bar{\rho})$ in the limit $J_k\bar{\rho}\rightarrow\infty$.

from the effective Hamiltonian (53) and the energy found from exact numerical diagonalization of Eq. (2) as a function of $J_k\bar{\rho}$ (at an arbitrary but fixed value $J_s/\bar{\delta}=0.52$). This energy difference ΔE should scale as $\propto 1/(J_k\bar{\rho})^5$, which is the next order correction beyond the accuracy considered here. The results shown in Fig. 3 confirm this scaling behavior and thereby the accuracy and completeness of our effective Hamiltonian. Similar results (not shown here) are found for other values of S_{tot} and for both even and odd number of electrons in the dot.

It is interesting to study the ground-state value of the total spin S_{tot} . This quantity was studied theoretically^{23,24,27} and can be probed experimentally.⁴⁰ The ground-state spin S_{tot} undergoes successive transitions to higher values (known as the Stoner staircase) when the exchange coupling constant J_s is varied between $J_s=0$ and $J_s\sim\bar{\delta}$. The transition steps in the Stoner staircase are shifted by the Kondo interaction. In Fig. 4 we show numerical results for the ground-state spin diagram in the two-dimensional parameter space of $J_s/\bar{\delta}, J_k\bar{\rho}$ for a particular mesoscopic realization of the single-particle Hamiltonian of the dot. The exact spin transition curves (colored lines) that separate regions of fixed ground-state spin S_{tot} are monotonically decreasing for $J_k\bar{\rho}\lesssim 1$ and monotonically increasing for $J_k\bar{\rho}\gtrsim 1$. Note also that for the particular mesoscopic realization chosen in Fig. 4, certain values of S_{tot} (e.g., $S_{\text{tot}}=1, 3$) never become the ground-state values of the total spin in the weak-coupling limit. In contrast, the ground-state spin assumes these values in the strong-coupling limit. Our analytical results in this limit, shown by the dashed lines in Fig. 4, are in very good agreement with the exact numerical results down to values of $J_k\bar{\rho}\approx 2$. The dotted black lines in Fig. 4 are the corresponding transition lines when we do not include interaction terms beyond the renormalized universal Hamiltonian of the reduced dot, i.e., when we assume the effective Hamiltonian to be given by $\eta+\tilde{H}'_d$ [see Eq.

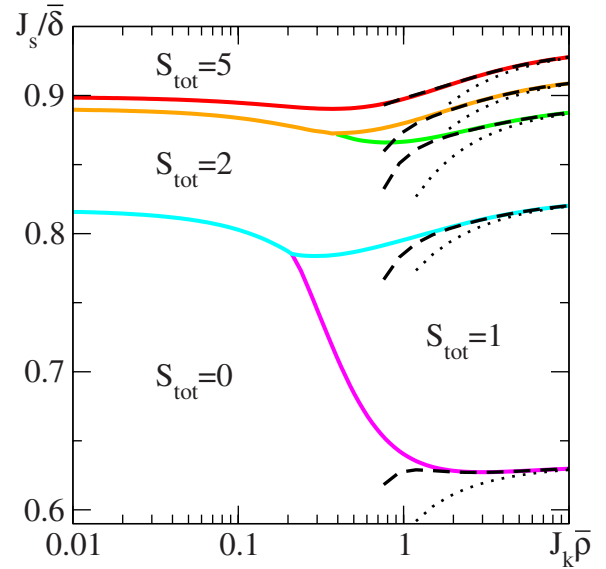


FIG. 4. (Color online) Ground-state spin S_{tot} of the system in Fig. 1 with finite exchange constant J_s and Kondo coupling J_k . We consider 11 electrons in a dot with $N=11$ single-particle levels, using an arbitrary random-matrix realization of the single-particle spectrum ε_n^0 but nonfluctuating orbital wave functions $\phi_n(0)=1/\sqrt{N}$. Lines show the transition curves separating regions of fixed S_{tot} . The estimates based on our strong-coupling expansion [Eq. (53)] for the Hamiltonian (dashed black lines) are compared with full numerical solutions (colored solid lines). The dotted black lines are the transition curves obtained when the strong-coupling limit is described by a renormalized universal Hamiltonian alone, i.e., $\tilde{H}^{\text{eff}}=\eta+\tilde{H}'_d$ in Eq. (53).

(53)]. These dotted curves converge much slower to the full numerical solutions (colored lines) than the dashed curves determined from the effective Hamiltonian (53). However, both the dashed and the dotted lines reproduce the monotonic increase of the exact transition curves with J_k for $J_k\bar{\rho}\gtrsim 2$. We conclude that this monotonic increase originates in the renormalization of the effective exchange-coupling constant in the reduced dot, $\tilde{J}_s\approx J_s(1+J_s/J_k+\dots)$, which is contained in the approximations used for both the dashed and the dotted lines. The renormalized exchange constant \tilde{J}_s decreases with increasing J_k causing the spin-transition curves to move upward with increasing J_k .

VI. DISCUSSION AND CONCLUSION

We have investigated the strong-coupling limit of the Kondo problem when the screening electrons reside in a large quantum dot that is described by the universal Hamiltonian. Unlike the conventional Kondo problem, the model considered here has a discrete single-particle spectrum and includes electron-electron interactions in the form of a ferromagnetic exchange interaction.

We have followed here a procedure that was originally proposed in Ref. 36 for the conventional Kondo problem in the absence of exchange correlations in the electron gas. As pointed out there, one can find the effective Hamiltonian at strong Kondo coupling ($T\ll T_K$) by considering the *bare*

strong-coupling limit $J_k \gg t_0$. This bare strong-coupling limit is the one for which we have now provided a closed expression of all effective interaction terms up to fourth order in t_0/J_k and J_s/J_k when the electron gas is described by the universal Hamiltonian. However, if the bandwidth D of this electron gas is very large $D \gg \bar{\delta}$, the limit of strong coupling can be effectively reached at much smaller values of J_k than those of the bare limit. For such a system with large bandwidth, the strong-coupling limit corresponds to a Kondo temperature T_K that is larger than the system's temperature and average level spacing, $T_K \gg T, \bar{\delta}$. An important insight in Kondo theory is that the effective Hamiltonians of both strong-coupling limits are related by a scaling analysis⁴¹ in which the Kondo Hamiltonian is renormalized by successive truncations of the bandwidth D , leaving the low-energy physics unchanged. As the reduced bandwidth $\tilde{D} \rightarrow 0$ (or equivalently $T \rightarrow 0$), the renormalized Kondo coupling constant diverges.⁴² The coupling constants of the various terms in the effective strong-coupling Hamiltonian are typically determined by fitting the lowest excitations of the effective Hamiltonian with those obtained by a numerical solution of the full problem. For a detailed review of this procedure see, e.g., Refs. 2, 42, and 43.

By deriving the effective Hamiltonian \hat{H}^{eff} for the *bare* strong-coupling limit [see Eq. (53)], we have completed successfully the first step in our goal to understand the strong-coupling limit of the Kondo problem in the presence of exchange correlations in the mesoscopic electron gas. We found that the exchange interaction in the universal Hamiltonian gives rise to two additional terms in \hat{H}^{eff} : a four-body contribution $\hat{\mathbf{S}}_d'^4$ that can be absorbed into a spin-dependent exchange coupling in the reduced dot, and an interaction term $\hat{\mathbf{s}}_1 \cdot \hat{\mathbf{S}}_d'$ that describes an exchange interaction between an electron in the vicinity of the Kondo spin and the total spin of the reduced dot. This term is induced by the virtual polarization of the Kondo singlet involving excursions to both the doublet and triplet subspaces. Unlike the conventional Kondo problem ($J_s=0$), this interaction is nonlocal as it involves the total spin of all sites of the electron gas (after the removal of an electron at site 0).

It would be of interest to identify similar interaction terms in the low-temperature behavior of a correlated Kondo state with a large bandwidth D . Our numerical diagonalization method of Ref. 27 is limited to a rather small bandwidth, e.g., $N=11$ levels for the results shown in Figs. 3 and 4. For such small bandwidths, the bare and renormalized strong-coupling limits essentially coincide, and we could use our numerical diagonalization method to validate the analytical derivations. For a numerical solution at larger bandwidths, a numerical renormalization group (NRG) technique⁴² might be useful. The challenge for NRG is the inclusion of nonlocal correlations induced by the exchange interaction in the universal Hamiltonian. With numerical solutions at hand, it would be interesting to investigate whether the renormalization of the large bandwidth Kondo problem induces any other “leading irrelevant” interaction terms around the strong-coupling fixed point beyond those we have identified here.

ACKNOWLEDGMENTS

We thank S. Adam, H. Baranger, L. Glazman, D. Goldhaber-Gordon, R. Kaul, K. Le Hur, G. Murthy, S. Schmidt, A. D. Stone, H. E. Türeci, and J. von Delft for helpful discussions. This work was supported in part by the Max-Kade Foundation, the W. M. Keck Foundation, U.S. DOE under Grant No. DE-FG-0291-ER-40608, and NSF under Grant No. DMR 0408636.

APPENDIX

In this appendix we provide various expressions that are useful for deriving the effective Hamiltonian. The notation used here follows the convention of Ref. 44.

The product of a hopping operator $\sum_{\sigma} \hat{c}_{1,\sigma}^{\dagger} \hat{c}_{0,\sigma}$ between sites 0 and 1 and its Hermitian conjugate can be expressed in terms of the occupation number (\hat{n}_0, \hat{n}_1) and spin ($\hat{\mathbf{s}}_0, \hat{\mathbf{s}}_1$) operators at these sites,

$$\sum_{\sigma, \sigma'} \hat{c}_{0,\sigma}^{\dagger} \hat{c}_{1,\sigma} \hat{c}_{1,\sigma'}^{\dagger} \hat{c}_{0,\sigma'} = \hat{n}_0(1 - \hat{n}_1/2) - 2\hat{\mathbf{s}}_0 \cdot \hat{\mathbf{s}}_1, \quad (\text{A1})$$

$$\sum_{\sigma, \sigma'} \hat{c}_{1,\sigma}^{\dagger} \hat{c}_{0,\sigma} \hat{c}_{0,\sigma'}^{\dagger} \hat{c}_{1,\sigma'} = \hat{n}_1(1 - \hat{n}_0/2) - 2\hat{\mathbf{s}}_0 \cdot \hat{\mathbf{s}}_1. \quad (\text{A2})$$

The spin raising and lowering operators, $\hat{S}_{\pm} \equiv \hat{S}_x \pm i\hat{S}_y$, satisfy, together with S_z , the usual su(2) commutation relations

$$[\hat{S}_z, \hat{S}_{\pm}] = \pm \hat{S}_{\pm}, \quad [\hat{S}_+, \hat{S}_-] = 2\hat{S}_z \quad (\text{A3})$$

while $\hat{\mathbf{S}}^2 = \hat{S}_z^2 + \frac{1}{2}(\hat{S}_+ \hat{S}_- + \hat{S}_- \hat{S}_+)$. The su(2) commutation relations for the cartesian components of the spin, $[\hat{S}_i, \hat{S}_j] = i\sum_k \epsilon_{ijk} \hat{S}_k$, can also be written in the form $\hat{\mathbf{S}} \times \hat{\mathbf{S}} = i\hat{\mathbf{S}}$. The triple scalar product of two spin operators, e.g., $\hat{\mathbf{S}}_d'$ and $\hat{\mathbf{s}}_1$ is then given by

$$\hat{\mathbf{S}}_d' \cdot (\hat{\mathbf{s}}_1 \times \hat{\mathbf{S}}_d') = i\hat{\mathbf{s}}_1 \cdot \hat{\mathbf{S}}_d'. \quad (\text{A4})$$

Other operator relations between $\hat{\mathbf{S}}_d'$ and operators on site 1 are

$$\hat{\mathbf{S}}_d'^2 \hat{c}_{1\pm} = \hat{c}_{1\pm} \hat{\mathbf{S}}_d'^2 + \frac{3\hat{c}_{1\pm}}{4} + \hat{c}_{1\mp} \hat{S}'_{d,\mp} \mp \hat{c}_{1\pm} \hat{S}'_{d,z}, \quad (\text{A5})$$

TABLE I. Matrix elements $\langle \psi_1 | \hat{O}_1 | \psi_2 \rangle$ of the operator $\hat{O}_1 = \hat{H}_{\text{hop}}^{(0,1)} \hat{H}_{\text{hop}}^{(0,1)} / |t_0|^2$. The corresponding states ψ_1 (ψ_2) are listed in the left column (top row), and are characterized by the quantum numbers $S_{K0}, S_{K0,z}$.

$\langle \psi_1 \hat{O}_1 \psi_2 \rangle$	$ 0, 0\rangle$	$ 1, -1\rangle$	$ 1, 0\rangle$	$ 1, +1\rangle$
$\langle 0, 0 $	1	$\sqrt{2}\hat{S}_{1,-}$	$2\hat{S}_{1,z}$	$-\sqrt{2}\hat{S}_{1,+}$
$\langle 1, -1 $	$\sqrt{2}\hat{S}_{1,+}$	$1 + 2\hat{S}_{1,z}$	$-\sqrt{2}\hat{S}_{1,+}$	0
$\langle 1, 0 $	$2\hat{S}_{1,z}$	$-\sqrt{2}\hat{S}_{1,-}$	1	$-\sqrt{2}\hat{S}_{1,+}$
$\langle 1, +1 $	$-\sqrt{2}\hat{S}_{1,-}$	0	$-\sqrt{2}\hat{S}_{1,-}$	$1 - 2\hat{S}_{1,z}$

TABLE II. Matrix elements $\langle \psi_1 | \hat{s}_0 \cdot \hat{S}'_d | \psi_2 \rangle$. Notation as in Table I.

$\langle \psi_1 \hat{s}_0 \cdot \hat{S}'_d \psi_2 \rangle$	$ 0,0\rangle$	$ 1,-1\rangle$	$ 1,0\rangle$	$ 1,+1\rangle$
$\langle 0,0 $	0	$-\hat{S}'_{d,-}/\sqrt{2}$	$-\hat{S}'_{d,z}$	$\hat{S}'_{d,+}/\sqrt{2}$
$\langle 1,-1 $	$-\hat{S}'_{d,+}/\sqrt{2}$	$-\hat{S}'_{d,z}$	$\hat{S}'_{d,+}/\sqrt{2}$	0
$\langle 1,0 $	$-\hat{S}'_{d,z}$	$\hat{S}'_{d,-}/\sqrt{2}$	0	$\hat{S}'_{d,+}/\sqrt{2}$
$\langle 1,+1 $	$\hat{S}'_{d,-}/\sqrt{2}$	0	$\hat{S}'_{d,-}/\sqrt{2}$	$+\hat{S}'_{d,z}$

$$\hat{S}'_d \hat{c}_{1\pm}^\dagger = \hat{c}_{1\pm}^\dagger \hat{S}'_d + \frac{3\hat{c}_{1\pm}^\dagger}{4} + \hat{c}_{1\pm}^\dagger \hat{S}'_{d,\pm} \pm \hat{c}_{1\pm}^\dagger \hat{S}'_{d,z}. \quad (\text{A6})$$

Useful relations involve the expectation values in the singlet state of observables at site 0

$$\langle \hat{c}_{0,\sigma}^\dagger \hat{c}_{0,\sigma'} \rangle_s = \langle \hat{c}_{0,\sigma'}^\dagger \hat{c}_{0,\sigma} \rangle_s = \frac{1}{2} \delta_{\sigma\sigma'}, \quad \langle \hat{n}_0 \rangle_s = 1, \quad (\text{A7})$$

$$\langle \hat{s}_{0,i} \rangle_s = 0, \quad (\text{A8})$$

$$\langle \hat{s}_{0,i} \hat{s}_{0,j} \rangle_s = \frac{1}{4} \delta_{ij}, \quad (\text{A9})$$

$$\langle \hat{s}_{0,i} \hat{s}_{0,j} \hat{s}_{0,k} \rangle_s = \frac{i}{8} \epsilon_{ijk}, \quad (\text{A10})$$

where $\hat{s}_{0,i}$ is the i th cartesian component of \hat{s}_0 and ϵ_{ijk} is the third rank antisymmetric tensor.

We can also derive the following expressions for singlet expectation values of the form $\langle \hat{H}_{sd} \dots \hat{H}_{sd} \rangle_s$,

TABLE III. Matrix elements $\langle \psi_1 | \hat{O}_2 | \psi_2 \rangle$ of the operator $\hat{O}_2 = \hat{H}_{\text{hop}}^{(0,1)} \hat{S}'_d \hat{H}_{\text{hop}}^{(0,1)} / |t_0|^2$. Notation as in Table I.

$\langle \psi_1 \hat{O}_2 \psi_2 \rangle$	$ 0,0\rangle$
$\langle 1,-1 $	$\frac{1}{2}(-\hat{c}_{1-} \hat{S}'_d \hat{c}_{1+}^\dagger + \hat{c}_{1+}^\dagger \hat{S}'_d \hat{c}_{1-})$
$\langle 1,0 $	$\frac{1}{2}(-\hat{c}_{1+} \hat{S}'_d \hat{c}_{1+}^\dagger + \hat{c}_{1-} \hat{S}'_d \hat{c}_{1-}^\dagger - \hat{c}_{1-}^\dagger \hat{S}'_d \hat{c}_{1-} + \hat{c}_{1+}^\dagger \hat{S}'_d \hat{c}_{1+})$
$\langle 1,+1 $	$\frac{1}{2}(\hat{c}_{1+} \hat{S}'_d \hat{c}_{1-}^\dagger - \hat{c}_{1-}^\dagger \hat{S}'_d \hat{c}_{1+})$

$$\langle \hat{H}_{sd} \hat{n}_0 \hat{H}_{ds} \rangle_s = |t_0|^2 \hat{n}_1, \quad (\text{A11})$$

$$\langle \hat{H}_{sd} \hat{n}_1 \hat{H}_{ds} \rangle_s = |t_0|^2, \quad (\text{A12})$$

$$\langle \hat{H}_{sd} \hat{n}_0^2 \hat{H}_{ds} \rangle_s = 2|t_0|^2 \hat{n}_1, \quad (\text{A13})$$

$$\langle \hat{H}_{sd} \hat{n}_1^2 \hat{H}_{ds} \rangle_s = |t_0|^2 (1 + \hat{n}_1 - 2\hat{n}_1 + \hat{n}_{1-}), \quad (\text{A14})$$

and

$$\langle \hat{H}_{sd} \hat{S}'_d \hat{H}_{ds} \rangle_s = |t_0|^2 \left(\frac{3}{4} + \hat{S}'_d{}^2 - 2\hat{s}_1 \cdot \hat{S}'_d \right), \quad (\text{A15})$$

$$\langle \hat{H}_{sd} \hat{S}'_d{}^4 \hat{H}_{ds} \rangle_s = |t_0|^2 \left(\hat{S}'_d{}^4 - 4\hat{s}_1 \cdot \hat{S}'_d \hat{S}'_d{}^2 - \hat{s}_1 \cdot \hat{S}'_d + \frac{5}{2} \hat{S}'_d{}^2 + \frac{9}{16} \right). \quad (\text{A16})$$

Matrix elements of various observables within and between the singlet and triplet manifolds are listed in Tables I–III.

¹J. Kondo, Prog. Theor. Phys. **32**, 37 (1964).

²A. C. Hewson, *The Kondo Problem to Heavy Fermions* (Cambridge University Press, Cambridge, England, 1993).

³L. Kouwenhoven and L. Glazman, Phys. World **14** (1), 33 (2001).

⁴D. Goldhaber-Gordon, H. Shtrikman, D. Mahalu, D. Abusch-Magder, U. Meirav, and M. A. Kastner, Nature (London) **391**, 156 (1998).

⁵S. M. Cronenwett, T. H. Oosterkamp, and L. Kouwenhoven, Science **281**, 540 (1998).

⁶J. Schmid, J. Weis, K. Eberl, and K. v. Klitzing, Physica B **256-258**, 182 (1998).

⁷F. Simmel, R. H. Blick, J. P. Kotthaus, W. Wegscheider, and M. Bichler, Phys. Rev. Lett. **83**, 804 (1999).

⁸W. G. van der Wiel, S. De Franceschi, T. Fujisawa, J. M. Elzerman, S. Tarucha, and L. P. Kouwenhoven, Science **289**, 2105 (2000).

⁹N. J. Craig, J. M. Taylor, E. A. Lester, C. M. Marcus, M. P. Hanson, and A. C. Gossard, Science **304**, 565 (2004).

¹⁰P. Jarillo-Herrero, J. Kong, H. S. J. van der Zant, C. Dekker, L. P. Kouwenhoven, and S. De Franceschi, Nature (London) **434**, 484 (2005).

¹¹R. M. Potok, I. G. Rau, H. Shtrikman, Y. Oreg, and D. Goldhaber-Gordon, Nature (London) **446**, 167 (2007).

¹²A. Hübel, K. Held, J. Weis, and K. v. Klitzing, Phys. Rev. Lett. **101**, 186804 (2008).

¹³M. R. Calvo, J. Fernández-Rossier, J. J. Palacios, D. Jacob, D. Natelson, and C. Untiedt, Nature (London) **458**, 1150 (2009).

¹⁴L. I. Glazman and M. E. Raikh, JETP Lett. **47**, 452 (1988).

¹⁵T. K. Ng and P. A. Lee, Phys. Rev. Lett. **61**, 1768 (1988).

¹⁶Y. Meir, N. S. Wingreen, and P. A. Lee, Phys. Rev. Lett. **66**, 3048 (1991); **70**, 2601 (1993).

¹⁷W. B. Thimm, J. Kroha, and J. von Delft, Phys. Rev. Lett. **82**, 2143 (1999).

¹⁸P. Simon and I. Affleck, Phys. Rev. B **64**, 085308 (2001).

¹⁹P. Simon and I. Affleck, Phys. Rev. Lett. **89**, 206602 (2002).

²⁰P. S. Cornaglia and C. A. Balseiro, Phys. Rev. Lett. **90**, 216801 (2003).

²¹M. Pustilnik and L. Glazman, J. Phys.: Condens. Matter **16**, R513 (2004).

²²R. K. Kaul, D. Ullmo, S. Chandrasekharan, and H. U. Baranger, Europhys. Lett. **71**, 973 (2005).

²³G. Murthy, Phys. Rev. Lett. **94**, 126803 (2005).

²⁴R. K. Kaul, G. Zarand, S. Chandrasekharan, D. Ullmo, and H. U.

- Baranger, Phys. Rev. Lett. **96**, 176802 (2006).
- ²⁵J. Martinek, M. Sindel, L. Borda, J. Barnaś, J. König, G. Schön, and J. von Delft, Phys. Rev. Lett. **91**, 247202 (2003).
- ²⁶P. Vitushinsky, A. A. Clerk, and K. Le Hur, Phys. Rev. Lett. **100**, 036603 (2008).
- ²⁷S. Rotter, H. E. Türeci, Y. Alhassid, and A. D. Stone, Phys. Rev. Lett. **100**, 166601 (2008).
- ²⁸R. A. Jalabert, A. D. Stone, and Y. Alhassid, Phys. Rev. Lett. **68**, 3468 (1992).
- ²⁹J. A. Folk, S. R. Patel, S. F. Godijn, A. G. Huibers, S. M. Cronenwett, C. M. Marcus, K. Campman, and A. C. Gossard, Phys. Rev. Lett. **76**, 1699 (1996).
- ³⁰A. M. Chang, H. U. Baranger, L. N. Pfeiffer, K. W. West, and T. Y. Chang, Phys. Rev. Lett. **76**, 1695 (1996).
- ³¹Y. Alhassid, Rev. Mod. Phys. **72**, 895 (2000).
- ³²A. V. Andreev and A. Kamenev, Phys. Rev. Lett. **81**, 3199 (1998); P. W. Brouwer, Y. Oreg, and B. I. Halperin, Phys. Rev. B **60**, R13977 (1999); H. U. Baranger, D. Ullmo, and L. I. Glazman, *ibid.* **61**, R2425 (2000); I. L. Kurland, I. L. Aleiner, and B. L. Altshuler, *ibid.* **62**, 14886 (2000).
- ³³Y. Alhassid and T. Rupp, Phys. Rev. Lett. **91**, 056801 (2003).
- ³⁴S. R. Patel, S. M. Cronenwett, D. R. Stewart, A. G. Huibers, C. M. Marcus, C. I. Duruöz, J. S. Harris, Jr., K. Campman, and A. C. Gossard, Phys. Rev. Lett. **80**, 4522 (1998); S. R. Patel, D. R. Stewart, C. M. Marcus, M. Gökçedağ, Y. Alhassid, A. D. Stone, C. I. Duruöz, and J. S. Harris, Jr., *ibid.* **81**, 5900 (1998).
- ³⁵M. J. Zuckermann, Solid State Commun. **9**, 1861 (1971); A. I. Larkin and V. I. Melnikov, Zh. Eksp. Teor. Fiz. **61**, 1231 (1971) [Sov. Phys. JETP **34**, 656 (1972)].
- ³⁶P. Nozières, J. Low Temp. Phys. **17**, 31 (1974).
- ³⁷H. E. Türeci and Y. Alhassid, Phys. Rev. B **74**, 165333 (2006).
- ³⁸P. Brouwer, *Lecture Notes on Solid State Physics* (Cornell University, Ithaca, 2004).
- ³⁹Since the exchange constant J_s is typically below $\sim \bar{\delta}$, the condition $J_k \gg J_s$ is automatically satisfied in the strong-coupling limit.
- ⁴⁰D. S. Duncan, D. Goldhaber-Gordon, R. M. Westervelt, K. D. Maranowski, and A. C. Gossard, Appl. Phys. Lett. **77**, 2183 (2000); J. A. Folk, C. M. Marcus, R. Berkovits, I. L. Kurland, I. L. Aleiner, and B. L. Altshuler, Phys. Scr. **T90**, 26 (2001); L. P. Kouwenhoven, D. G. Austing, and S. Tarucha, Rep. Prog. Phys. **64**, 701 (2001); S. Lindemann, T. Ihn, T. Heinzel, W. Zwerger, K. Ensslin, K. Maranowski, and A. C. Gossard, Phys. Rev. B **66**, 195314 (2002); R. M. Potok, J. A. Folk, C. M. Marcus, V. Umansky, M. Hanson, and A. C. Gossard, Phys. Rev. Lett. **91**, 016802 (2003); R. Hanson, L. P. Kouwenhoven, J. R. Petta, S. Tarucha, and L. M. K. Vandersypen, Rev. Mod. Phys. **79**, 1217 (2007).
- ⁴¹P. W. Anderson, J. Phys. C **3**, 2436 (1970).
- ⁴²K. G. Wilson, Rev. Mod. Phys. **47**, 773 (1975).
- ⁴³P. Nozières, *Conference Proceedings on Low Temperature Physics-LT 14*, edited by M. Krusius and M. Vuorio (North-Holland, Amsterdam, 1975), Vol. 5, p. 339.
- ⁴⁴A. Messiah, *Quantum Mechanics* (North-Holland, Amsterdam, 1961), Vol. II, Appendix C.